Science and Technology Journal Vol. 12 Issue: 2 June 2024 ISSN: 2321-3388

Velocity and Energy Distribution at Corrugated Interface of Monoclinic Medium

Lalvohbika Jongte[1], Lianngenga Rengsi[2], and Lalhriattira Fanai[3]
[1,2,3]Department of Mathematics and Computer Science, Mizoram University, Aizawl-796004, India
E-mail: [1]vohbikajongte@gmail.com, [2]rengsi.9@gmail.com, [3]fanailalhriattira@gmail.com
*Corresponding Author

Abstract—This paper investigates how elastic waves reflect and transmit when a plane *qSV*-wave encounters a corrugated interface between two different monoclinic elastic half-spaces. The corrugations on the interface lead to the generation of both regular and irregular reflected and transmitted waves, each traveling at distinct phase velocities. The study aims to determine the velocities and energy ratios of these waves, which are affected by various factors including the angle of incidence, the elastic constants of the materials, the properties of the interface's corrugation, and the frequency parameter. To analyse the problem, we performed computations for a specific model $x_3 = d\cos(px_2)$, obtaining the velocities and energy ratios. The paper also discusses the influence of corrugation and the frequency parameter on these quantities.

Keywords: Reflection, transmission, corrugated, monoclinic, velocity, energy ratio.

INTRODUCTION

Elastic wave propagation is utilized in various domains, including seismology and earthquake engineering, Non-Destructive Testing (NDT), medical imaging (such as ultrasonography), telecommunications, and geotechnical engineering. Elastic waves arise whenever there is a sudden stress imbalance within or on the surface of an elastic medium. Virtually any abrupt deformation or displacement within the medium triggers such waves (Lay and Wallace 1995). Among natural phenomena, earthquakes stand out as significant sources, with the analysis of the waves they propagate being pivotal in enhancing our comprehension of the earth's internal composition and the mechanisms underlying seismic events (Pujol 2003). The release of energy at the source of the earthquake and propagate through the earth generates the seismic waves which carry valuable information about the event and the subsurface. The velocity, amplitude, and energy ratios of seismic waves have profound effects on seismic wave propagation. These parameters influence wave speed, refraction, reflection, attenuation, energy transfer, damage potential, signal detection, and energy partitioning. Understanding and analysing these effects are crucial for seismology, earthquake engineering, and subsurface exploration.

Numerous scholars have undertaken research on the circumstances of reflection and refraction at corrugated interfaces, and this area of study continues to captivate their interest. Several notable findings concerning the behaviour of reflection and transmission at corrugated interfaces, as well as within monoclinic materials, have already been published. From the paper of *On the dynamical theory of gratings*, Rayleigh (1907) investigated the waves propagation on a regularly corrugated surface and he observed that the depth of the corrugations is small in comparision with the length of the waves. Rice (1951) studied the reflection of electromagnetic waves from a rough or corrugated surface, and found that the Fourier components of the surface waves whose wavelengths are much greater than that of the electromagnetic wave tends to produce attenuation through scattering, while the

 https://doi.org/10.22232/stj.2024.12.02.09

guiding action of the surface is due to the components of shorter wavelength. From the investigation of the reflection of elastic waves at the corrugated surface, Sato (1955) observed that when the wavelength of the corrugations become large, the reflected waves exhibit an increase in the number of spectral components. In the study by Abubakar (1962), the scattering of *qSV* and *qP* waves at a rough boundary surface was examined. The researcher found that the reflected waves include both specularly reflected waves and several diffracted waves, which propagate in horizontal directions, then this effect is particularly pronounced when the wavelength of the incident wave is much larger than that of the surface wave. In addition to the specularly reflected *P* and *SV* -waves, whose amplitudes are independent of the surface's curvature, there are scattered waves traveling in various directions (Abubakar 1963). By applying the Rayleigh's procedure, Asano (1960, 1961) also observed that the effect of corrugated interface on reflection is larger than that on the refraction of elastic waves. Levy and Deresiewicz (1967) expanded upon Asano's research work by examining a layered medium with irregular internal interfaces. They observed that for the case of a corrugated bottom surface, the reflection and transmission amplitudes exhibit the same qualitative features as the transmission and reflection amplitudes, respectively, due to a corrugated top surface. Paul and Campillo (1988) conducted an investigation into the influence of minor-scale irregularities on elastic wave reflections at a corrugated interface. Their findings indicated that the presence of these irregularities scarcely affects the intensity of reflected *P* waves. In monoclinic media, for plane waves propagating in arbitrary directions within the plane of symmetry, *SH* waves are transverse, while *SV* waves are not purely transverse, and *P* waves are not purely longitudinal. This implies that pure longitudinal and pure transverse waves can only propagate in specific directions (Singh 1999; Singh and Khurana 2001).

The reflection coefficient plays an important role in the study of wave propagation. It helps to understand how waves behave when encountering interfaces or boundaries between different media. The reflection coefficient quantifies the portion of an incident wave that gets reflected back upon encountering such a boundary. The transmission coefficient is employed when analyzing wave propagation in a medium with discontinuities. It characterizes the amplitude, intensity, or total power of the transmitted wave in relation to the incident wave. Nayfeh (1991) derived the expressions for the reflection and transmission coefficients in the isotropic media and examined the behaviour of these coefficients for varying angle of incidence and propagation direction angles. The reflection coefficients of *P* and *SV*-waves in a monoclinic media was derived by Chattopadhyay and Choudhury (1995), they also observed that this medium have significant effect on the reflection coefficients. When the waves propagated in a monoclinic medium, the material constants have a considerable effect on the reflection and transmission coefficients of *P* and *SV*-waves (Chattopadhyay and Saha 1996). In the study conducted by Saha *et al*. (2020), they examined the behaviour of reflection and refraction of a plane wave at the interface between two functionally graded incompressible monoclinic media. The analysis took into account on the influence of initial stress and the presence or absence of gravity in each medium. The reflection and transmission coefficients of *SH*-waves at a corrugated interface between two anisotropic and between two monoclinic elastic half spaces are investigated separately by Tomar and Kaur (2003, 2007). They found that the impact of these coefficients on transverse isotropy is greatest at normal incidence. Additionally, the reflection and transmission coefficients are significantly affected by both the surface corrugation and the elastic properties of the media. They also studied the propagation of shear waves at a corrugated interface between anisotropic elastic and visco-elastic solid half-spaces, and then found that the effect of reflection and transmission coefficients are minimum near the normal incidence and maximum near the grazing incidence (Tomar and Kaur 2007). The reflection and transmission coefficients of *qP*-waves at a corrugated interface between two different elastic half-spaces of monoclinic type are derived by Singh and Tomar (2007), and observed that the coefficients corresponding to regularly reflected and transmitted waves are found to be greater than that of the irregularly reflected and transmitted waves. In a corrugated interface between two dissimilar pre-stressed elastic half spaces, the coefficients corresponding to irregularly reflected and transmitted waves are proportional to the amplitude of the corrugated interface and are also influenced significantly by the initial stresses of the half-spaces (Singh and Tomar 2008). Yu and Dravinski (2009) investigated the plain strain model for scattering of elastic waves by a completely embedded scatterer with a rough surface. Other research papers concerning the reflection and transmission of waves at free and rigid boundaries, as well as at the corrugated nature of different medium were

published by Mciver and Urka (1995), Mandal and Das (1996), Chattopadhyay *et al.* (1996), Singh and Lalvohbika (2018), Pandit *et al.* (2017), Prasad *et al.* (2017), Hermans (2003), Lalvohbika and Singh (2019), Singh *et al.* (2020), Gupta *et al.* (2022).

This paper aims to determine the phase velocities of waves and the energy distribution related to the reflection and transmission of elastic waves when a plane *qSV*-wave encounters a corrugated interface between two different monoclinic elastic half-spaces. The velocities and energy ratios are influenced by various factors, including the angle of incidence, the materials' elastic constants, the characteristics of the interface's corrugation, and the frequency parameters. To analyze this, we computed the velocities and energy ratios for a specific model and then examined how the corrugation and frequency parameters affect these quantities.

GOVERNING EQUATION

In a homogeneous anisotropic elastic material of monoclinic type, the consecutive relations with the x_2x_3-plane are given by (Singh and Khurana 2001)

$$T_{ii} = \sum_{j=1}^{3} c_{ij}e_{jj} + 2c_{i4}e_{23}, i = 1,2,3,$$

$$T_{12} = 2(c_{55}e_{13} + c_{56}e_{12}),\ T_{13} = 2(c_{56}e_{13} + c_{66}e_{12}),\ T_{23} = \sum_{k=1}^{4} c_{k4}e_{kk} + 2c_{44}e_{23} \quad (1)$$

where T_{ij}, for *i, j = 1, 2, 3* are stress tensors, c_{ij}, for *i, j = 1, 2, ..., 5, 6* are elastic constants and e_{ij} is the strain tensor given by

$$2e_{ij} = u_{i,j} + u_{j,i},$$

The equation of motion without body forces are given by

$$T_{ij,j} = \rho\frac{\partial^2 u_i}{\partial t^2}, \quad (i,j = 1,2,3) \quad (2)$$

where u_i are components of displacement and ρ is density of the medium.

Now, considering two dimensional wave propagation in the x_2x_3-plane so that

$$u_1 = 0 \ \text{ and } \ u_{i,1} \equiv 0 \quad (3)$$

By using (3) and the stress tensors of (1), the equations of motion (2) may be written as

$$c_{22}\frac{\partial^2 u_2}{\partial x_2^2} + c_{44}\frac{\partial^2 u_2}{\partial x_3^2} + c_{24}\frac{\partial^2 u_3}{\partial x_2^2} + c_{34}\frac{\partial^2 u_3}{\partial x_3^2} + 2c_{24}\frac{\partial^2 u_2}{\partial x_2 x_3} + (c_{23} + c_{24})\frac{\partial^2 u_3}{\partial x_2 x_3} = \rho\frac{\partial^2 u_2}{\partial t^2}, \quad (4)$$

$$c_{24}\frac{\partial^2 u_2}{\partial x_2^2} + c_{34}\frac{\partial^2 u_2}{\partial x_3^2} + c_{44}\frac{\partial^2 u_3}{\partial x_2^2} + c_{33}\frac{\partial^2 u_3}{\partial x_3^2} + 2c_{34}\frac{\partial^2 u_3}{\partial x_2 x_3} + (c_{23} + c_{24})\frac{\partial^2 u_2}{\partial x_2 x_3} = \rho\frac{\partial^2 u_3}{\partial t^2}. \quad (5)$$

The solution of these Eqs. (4) and (5) may take in the form

$$\{u_2, u_3\} = \{Ad_2, Ad_3\}e^{ik(vt - p_2x_2 - p_3x_3)}, \quad (6)$$

where A is the amplitude, v is the phase velocity, k is the wave number, p_i is the unit propagation vector and d_i is the unit displacement vector. Using the displacement components u_2 and u_3 of (6) in (4) and (5), we have the velocity equation

$$v_{1,2} = \sqrt{\frac{\Lambda + \Theta \pm \sqrt{(\Lambda - \Theta)^2 + 4\Xi^2}}{2\rho}}, \quad (7)$$

where,

$$\Lambda = c_{22}p_2^2 + c_{44}p_3^2 + 2c_{34}p_2p_3,$$
$$\Xi = c_{24}p_2^2 + c_{34}p_3^2 + (c_{23} + c_{44})p_2p_3,$$
$$\Theta = c_{44}p_2^2 + c_{33}p_3^2 + 2c_{34}p_2p_3. \quad (8)$$

Here, v_1 and v_2 represents the phase velocity of *qP* and *qSV*-waves respectively.

SOLUTION AND FORMULATION OF THE PROBLEM

Consider the Cartesian coordinate system in x_2x_3-plane where x_1 and x_2-axis are lying horizontally, and the x_3-axis perpendicular to the x_1x_2-plane. The two dissimilar homogeneous monoclinic elastic half-spaces are denoted as $\mathcal{M} = \{(x_2, x_3) : x_2 \epsilon R, x_3 \epsilon [\xi, \infty)\}$ and $\mathcal{M}' = \{(x_2, x_3) : x_2 \epsilon R, x_3 \epsilon (-\infty, \xi)\}$. In this context, $x_3 = \xi(x_2)$ defines the separation between the two half-spaces, where $\xi(x_2)$ is a periodic function of x_2 that is independent of x_1 and has a mean value of zero. The elastic constants, stress tensors, and displacement components in medium $\mathcal{M}'$ are indicated with primes, while those in medium $\mathcal{M}$ are shown without primes. The Fourier series expansion of $\xi(x_2)$ is provided as follows

$$\xi(x_2) = \sum_{n=1}^{\infty}(\xi_n e^{inpx_2} + \xi_{-n}e^{-inpx_2}), \quad (9)$$

where $\xi_{\pm n}$ are the coefficients of series expansion of order n, p is the wave number and $\imath = \sqrt{-1}$.

Let us consider the reflection and transmission of elastic waves resulting from the incidence of a plane *qSV*-wave at the corrugated interface $x_3 = \xi(x_2)$. We assume that a plane *qSV*-wave is propagating within the half-space $\mathcal{M}$ at an angle θ_0 with a constant amplitude $\mathcal{A}_0$. Due to irregular interface, this incident wave generates both regularly and

irregularly reflected waves, as well as transmitted waves of *qSV* and *qP* types. The displacement components of reflected and transmitted waves for the half-space $\mathcal{M}$ and $\mathcal{M}'$ are given by

$$u_2 = \mathcal{A}_o e^{\mathcal{P}_0} + \mathcal{A}_1 e^{\mathcal{P}} + \mathcal{A}_2 e^{\mathcal{Q}} + \sum_{n=1}^{\infty} \{\mathcal{A}_{1n}^{\pm} e^{\mathcal{P}_n^{\pm}} + \mathcal{A}_{2n}^{\pm} e^{\mathcal{Q}_n^{\pm}}\} \quad (10)$$

$$u_3 = \mathcal{B}_o e^{\mathcal{P}_0} + \mathcal{B}_1 e^{\mathcal{P}} + \mathcal{B}_2 e^{\mathcal{Q}} + \sum_{n=1}^{\infty} \{\mathcal{B}_{1n}^{\pm} e^{\mathcal{P}_n^{\pm}} + \mathcal{B}_{2n}^{\pm} e^{\mathcal{Q}_n^{\pm}}\} \quad (11)$$

$$u_{2'} = \mathcal{A}_3 e^{\mathcal{R}} + \mathcal{A}_4 e^{\mathcal{S}} + \sum_{n=1}^{\infty} \{\mathcal{A}_{3n}^{\pm} e^{\mathcal{R}_n^{\pm}} + \mathcal{A}_{4n}^{\pm} e^{\mathcal{S}_n^{\pm}}\}, \quad (12)$$

$$u_{3'} = \mathcal{B}_3 e^{\mathcal{R}} + \mathcal{B}_4 e^{\mathcal{S}} + \sum_{n=1}^{\infty} \{\mathcal{B}_{3n}^{\pm} e^{\mathcal{R}_n^{\pm}} + \mathcal{B}_{4n}^{\pm} e^{\mathcal{S}_n^{\pm}}\}, \quad (13)$$

where $(\mathcal{A}_1, \mathcal{B}_1)$ and $(\mathcal{A}_2, \mathcal{B}_2)$, are amplitude constants of the regularly reflected *qSV* and *qP*-waves at an angle θ_1 and θ_2 respectively, $(\mathcal{A}_{1n}^{\pm}, \mathcal{B}_{1n}^{\pm})$ and $(\mathcal{A}_{2n}^{\pm}, \mathcal{B}_{2n}^{\pm})$ are amplitude constants of the irregularly reflected *qSV* and *qP*-waves at an angle $\theta_{1n}^{\pm}$ and $\theta_{2n}^{\pm}$ respectively, $(\mathcal{A}_3, \mathcal{B}_3)$ and $(\mathcal{A}_4, \mathcal{B}_4)$ are amplitude constants of the regularly transmitted *qSV* and *qP*-waves at an angle θ_3 and θ_4 respectively, $(\mathcal{A}_{3n}^{\pm}, \mathcal{B}_{3n}^{\pm})$ and $(\mathcal{A}_{4n}^{\pm}, \mathcal{B}_{4n}^{\pm})$ are amplitude constants of irregularly transmitted *qSV* and *qP*-waves at angles $\theta_{3n}^{\pm}$ and $\theta_{4n}^{\pm}$ respectively.

The expressions of $\mathcal{P}_0, \mathcal{P}, \mathcal{P}_n^{\pm}, \mathcal{Q}, \mathcal{Q}_n^{\pm}, \mathcal{R}, \mathcal{R}_n^{\pm}, \mathcal{S}, \mathcal{S}_n^{\pm}$ are given as :

$$\mathcal{P}_0 = \iota k_0(v_0 t - x_2 sin\theta_0 + x_3 cos\theta_0), \mathcal{P} = \iota k_1(v_1 t - x_2 sin\theta_1 - x_3 cos\theta_1),$$
$$\mathcal{P}_n^{\pm} = \iota k_1(v_2 t - x_2 sin\theta_{1n}^{\pm} - x_3 cos\theta_{1n}^{\pm})$$
$$\mathcal{Q} = \iota k_2(v_1 t - x_2 sin\theta_2 - x_3 cos\theta_2), \quad \mathcal{Q}_n^{\pm} = \iota k_2(v_1 t - x_2 sin\theta_{2n}^{\pm} - x_3 cos\theta_{2n}^{\pm}),$$
$$\mathcal{R} = \iota k_{1'}(v_4 t - x_2 sin\theta_3 + x_3 cos\theta_3), \quad \mathcal{R}_n^{\pm} = \iota k_{1'}(v_4 t - x_2 sin\theta_{3n}^{\pm} + x_3 cos\theta_{3n}^{\pm}),$$
$$\mathcal{S} = \iota k_{2'}(v_3 t - x_2 sin\theta_4 + x_3 cos\theta_4), \quad \mathcal{S}_n^{\pm} = \iota k_{2'}(v_3 t - x_2 sin\theta_{4n}^{\pm} + x_3 cos\theta_{4n}^{\pm}). \quad (14)$$

The amplitude constants for reflection and transmission of the incident *qSV*-waves satisfy the following relations (Singh and Khurana 2001)

$$\mathcal{A}_0 = \Pi_0 \mathcal{B}_0, \quad \mathcal{A}_i = \Pi_i \mathcal{B}_i, \quad \mathcal{A}_{in}^{\pm} = \Pi_{3i}^{\pm} \mathcal{B}_{3i}^{\pm}, \quad i = 1,2,3,4, \quad (15)$$

where,

$$\Pi_0 = \frac{\Xi_0}{\rho v_0^2 - \Lambda_0}, \quad \Pi_i = \frac{\Xi_i}{\rho v_j^2 - \Lambda_i}, \quad \Pi_{in}^{\pm} = \frac{\Xi_{in}^{\pm}}{\rho v_j^2 - \Lambda_{in}^{\pm}}, i,j = 1,2, i \neq j,$$

$$\Pi_i = \frac{\Xi_i}{\rho' v_j^2 - \Lambda_i}, \quad \Pi_{in}^{\pm} = \frac{\Xi_{in}^{\pm}}{\rho' v_j^2 - \Lambda_{in}^{\pm}}, i,j = 3,4, i \neq j.$$

From Eq. (7), the velocity of incident, reflected and transmitted waves are given by

$$v_0 = \sqrt{\frac{\Lambda_0 + \Theta_0 - \sqrt{(\Lambda_0 - \Theta_0)^2 + 4\Xi_0^2}}{2\rho}},$$

$$v_i = \sqrt{\frac{\Lambda_i + \Theta_i \pm \sqrt{(\Lambda_i - \Theta_i)^2 + 4\Xi_i^2}}{2\rho}},$$

$$v_j = \sqrt{\frac{\Lambda_j + \Theta_j \pm \sqrt{(\Lambda_j - \Theta_j)^2 + 4(\Xi_j)^2}}{2\rho'}},$$

where $i = 1,2, j = 3,4$.

Using the values of Eqs. (14) and (15) into Eqs. (10)-(13), the displacement components can be written as below

$$u_2 = [\Pi_0 \mathcal{B}_0 e^{\iota\xi K_0} + \Pi_1 \mathcal{B}_1 e^{-\iota\xi K_1} + \Pi_2 \mathcal{B}_2 e^{-\iota\xi K_2} + \sum_{n=1}^{\infty} \Pi_{1n}^{\pm} \mathcal{B}_{1n}^{\pm} e^{\mp \iota m p x_2} e^{-\iota\xi K_{1n}^{\pm}} + \sum_{n=1}^{\infty} \Pi_{2n}^{\pm} \mathcal{B}_{2n}^{\pm} e^{\mp \iota m p x_2} e^{-\iota\xi K_{2n}^{\pm}}] e^{\iota(\omega t - P_0 x_2)}, \quad (16)$$

$$u_3 = [\mathcal{B}_0 e^{\iota\xi K_0} + \mathcal{B}_1 e^{-\iota\xi K_1} + \mathcal{B}_2 e^{-\iota\xi K_2} + \sum_{n=1}^{\infty} \mathcal{B}_{1n}^{\pm} e^{\mp \iota m p x_2} e^{-\iota\xi K_{1n}^{\pm}} + \sum_{n=1}^{\infty} \mathcal{B}_{2n}^{\pm} e^{\mp \iota m p x_2} e^{-\iota\xi K_{2n}^{\pm}}] e^{\iota(\omega t - P_0 x_2)}, \quad (17)$$

$$u_2' = [\Pi_3 \mathcal{B}_3 e^{\iota\xi K_3} + \Pi_4 \mathcal{B}_4 e^{\iota\xi K_4} + \sum_{n=1}^{\infty} \Pi_{3n}^{\pm} \mathcal{B}_{3n}^{\pm} e^{\mp \iota m p x_2} e^{\iota\xi K_{3n}^{\pm}} + \sum_{n=1}^{\infty} \Pi_{4n}^{\pm} \mathcal{B}_{4n}^{\pm} e^{\mp \iota m p x_2} e^{\iota\xi K_{4n}^{\pm}}] e^{\iota(\omega t - P_0 x_2)}, \quad (18)$$

$$u_3' = [\mathcal{B}_3 e^{\iota\xi K_3} + \mathcal{B}_4 e^{\iota\xi K_4} + \sum_{n=1}^{\infty} \mathcal{B}_{3n}^{\pm} e^{\mp \iota m p x_2} e^{\iota\xi K_{3n}^{\pm}} + \sum_{n=1}^{\infty} \mathcal{B}_{4n}^{\pm} e^{\mp \iota m p x_2} e^{\iota\xi K_{4n}^{\pm}}] e^{\iota(\omega t - P_0 x_2)}, \quad (19)$$

where, $P_0 = \frac{\omega sin\theta_0}{v_0}, \quad K_0 = \frac{\omega cos\theta_0}{v_0}, \quad K_i = \frac{\omega cos\theta_i}{v_j},$

$$K_{in}^{\pm} = \frac{\omega cos\theta_{in}^{\pm}}{v_i}, \quad i,j = 1,2, \; i \neq j.$$

$$K_j = \frac{\omega cos\theta_j}{v_i}, \quad K_{jn}^{\pm} = \frac{\omega cos\theta_{jn}^{\pm}}{v_i}, \quad i,j = 3,4, \; i \neq j.$$

BOUNDARY CONDITIONS

The boundary conditions at the corrugated interface require the continuity of both displacements and tractions (including normal and shear components), as described below

$$u_2 = u_{2'}, \quad u_3 = u_{3'}, \quad (20)$$

$$T_{32} + (T_{33} - T_{22})\xi' - T_{23}\xi'^2 = T_{32}' + (T_{33}' - T_{22}')\xi' - T_{23}'\xi'^2, \quad (21)$$

$$T_{33} - 2T_{23}\xi' + T_{22}\xi'^2 = T_{33}' - 2T_{23}'\xi' + T_{22}'\xi'^2, \quad (22)$$

where ξ' is the derivatives of ξ with respect to x_2.

Considering the corrugated interface's amplitude to be extremely small, we can disregard higher powers of ξ, as

follows

$$e^{\pm\iota\xi K_0} = 1 \pm \iota\xi K_0 - 0\left(\xi^2\right),\ e^{\pm\iota\xi K_1} = 1 \pm \iota\xi K_1 - 0\left(\xi^2\right). \tag{23}$$

Using Eqs. (16)-(19) and (23), we obtain a set of equations from the above boundary conditions (20)-(22) (Singh and Lalvohbika 2018)

$$\Im\Re = \nabla \quad \text{and} \quad \Im^{\mp}\Re^{\mp} = \nabla^{\mp}, \tag{24}$$

where,

$$\Im = \begin{bmatrix} 1 & 1 & -1 & -1 \\ \Pi_1 & \Pi_2 & -\Pi_3 & -\Pi_4 \\ y_1 & y_2 & -y_3 & -y_4 \\ z_1 & z_2 & -z_3 & -z_4 \end{bmatrix},\ \Re = \begin{bmatrix} \mathcal{B}_1/\mathcal{B}_0 \\ \mathcal{B}_2/\mathcal{B}_0 \\ \mathcal{B}_3/\mathcal{B}_0 \\ \mathcal{B}_4/\mathcal{B}_0 \end{bmatrix},\ \nabla = \begin{bmatrix} -1 \\ -\Pi_0 \\ -y_0 \\ -z_0 \end{bmatrix},$$

$$\Im^{\mp} = \begin{bmatrix} 1 & 1 & -1 & -1 \\ \Pi_{1n}^{\pm} & \Pi_{2n}^{\pm} & -\Pi_{3n}^{\pm} & -\Pi_{4n}^{\pm} \\ \kappa_5^{\mp} & \kappa_6^{\mp} & -\kappa_7^{\mp} & -\kappa_8^{\mp} \\ \Phi_5^{\mp} & \Phi_6^{\mp} & -\Phi_7^{\mp} & -\Phi_8^{\mp} \end{bmatrix},\ \Re^{\mp} = \begin{bmatrix} \mathcal{B}_{1n}^{\pm}/\mathcal{B}_0 \\ \mathcal{B}_{2n}^{\pm}/\mathcal{B}_0 \\ \mathcal{B}_{3n}^{\pm}/\mathcal{B}_0 \\ \mathcal{B}_{4n}^{\pm}/\mathcal{B}_0 \end{bmatrix},\ \nabla^{\mp} = \begin{bmatrix} \zeta_1^{\mp} \\ \zeta_2^{\mp} \\ \zeta_3^{\mp} \\ \zeta_4 \mp \end{bmatrix},$$

$$y_0 = (\Pi_0 c_{24} + c_{44})P_0 - (\Pi_0 c_{44} + c_{34})K_0,$$

$$y_i = \begin{cases} (\Pi_i c_{24} + c_{44})P_0 + (\Pi_i c_{44} + c_{34})K_i, & i = 1,2 \\ (\Pi_i c'_{24} + c'_{44})P_0 - (\Pi_i c'_{44} + c'_{34})K_i, & i = 3,4 \end{cases},$$

$$\zeta_1^{\mp} = \iota\xi_{\mp n}\left[-K_0 + \sum_{i=1}^{4} K_i \frac{\mathcal{B}_i}{\mathcal{B}_0}\right],$$

$$\zeta_3^{\mp} = \iota\left[\kappa_0^{\mp} + \kappa_1^{\mp}\frac{\mathcal{B}_1}{\mathcal{B}_0} + \kappa_2^{\mp}\frac{\mathcal{B}_2}{\mathcal{B}_0} - \kappa_3^{\mp}\frac{\mathcal{B}_3}{\mathcal{B}_0} - \kappa_4^{\mp}\frac{\mathcal{B}_4}{\mathcal{B}_0}\right],$$

$$z_0 = (\Pi_0 c_{23} + c_{34})P_0 - (\Pi_0 c_{34} + c_{33})K_0,$$

$$z_i = \begin{cases} (\Pi_i c_{23} + c_{34})P_0 + (\Pi_i c_{34} + c_{33})K_i, & i = 1,2 \\ (\Pi_i c'_{24} + c'_{44})P_0 - (\Pi_i c'_{44} + c'_{34})K_i, & i = 3,4 \end{cases},$$

$$\zeta_2^{\mp} = \iota\xi_{\mp n}\left[-\Pi_0 K_0 + \sum_{i=1}^{4} \Pi_i K_i \frac{\mathcal{B}_i}{\mathcal{B}_0}\right],$$

$$\zeta_4^{\mp} = \iota\left[\Phi_0^{\mp} + \Phi_1^{\mp}\frac{\mathcal{B}_1}{\mathcal{B}_0} + \Phi_2^{\mp}\frac{\mathcal{B}_2}{\mathcal{B}_0} - \Phi_3^{\mp}\frac{\mathcal{B}_3}{\mathcal{B}_0} - \Phi_4^{\mp}\frac{\mathcal{B}_4}{\mathcal{B}_0}\right],$$

$$\kappa_0^{\mp} = [\{\mp(c_{23} - c_{22})npP_0 + c_{24}P_0K_0 \pm (c_{34} - c_{24})npK_0 - c_{44}K_0^2\}\Pi_0 \pm (c_{33} - c_{23})npK_0 - c_{34}K_0^2 \mp (c_{34} - c_{24})npP_0 + c_{44}P_0K_0]\xi_{\mp n},$$

$$\kappa_1^{\mp} = [\{\mp(c_{23} - c_{22})npP_0 - c_{24}P_0K_1 \pm (c_{34} - c_{24})npK_1 - c_{44}K_1^2\}\Pi_1 \pm (c_{33} - c_{23})npK_1 - c_{34}K_1^2 \mp (c_{34} - c_{24})npP_0 - c_{44}P_0K_1]\xi_{\mp n},$$

$$\kappa_2^{\mp} = [\{\mp(c_{23} - c_{22})npP_0 - c_{24}P_0K_2 \pm (c_{34} - c_{24})npK_2 - c_{44}K_2^2\}\Pi_2 \pm (c_{33} - c_{23})npK_2 - c_{34}K_2^2 \mp (c_{34} - c_{24})npP_0 - c_{44}P_0K_2]\xi_{\mp n},$$

$$\kappa_3^{\mp} = [\{\mp(c'_{23} - c'_{22})npP_0 + c'_{24}P_0K_3 \pm (c'_{34} - c'_{24})npK_3 - c'_{44}K_3^2\}\Pi_3 \pm (c'_{33} - c'_{23})npK_3 - c'_{34}K_3^2 \mp (c'_{34} - c'_{24})npP_0 + c'_{44}P_0K_3]\xi_{\mp n},$$

$$\kappa_4^{\mp} = [\{\mp(c'_{23} - c'_{22})npP_0 + c'_{24}P_0K_4 \pm (c'_{34} - c'_{24})npK_4 - c'_{44}K_4^2\}\Pi_4 \pm (c'_{33} - c'_{23})npK_4 - c'_{34}K_4^2 \mp (c'_{34} - c'_{24})npP_0 + c'_{44}P_0K_4]\xi_{\mp n},$$

$$\kappa_5^{\mp} = -\left[\left\{c_{44}K_{1n}^{\pm} + c_{24}\left(P_0 \pm np\right)\right\}\Pi_{1n}^{\pm} + c_{34}K_{1n}^{\pm} + c_{44}\left(P_0 \pm np\right)\right],$$

$$\kappa_6^{\mp} = -\left[\left\{c_{44}K_{2n}^{\pm} + c_{24}\left(P_0 \pm np\right)\right\}\Pi_{2n}^{\pm} + c_{34}K_{2n}^{\pm} + c_{44}\left(P_0 \pm np\right)\right],$$

$$\kappa_7^{\mp} = \left\{c'_{44}K_{3n}^{\pm} - c'_{24}\left(P_0 \pm np\right)\right\}\Pi_{3n}^{\pm} + c'_{34}K_{3n}^{\pm} - c'_{44}\left(P_0 \pm np\right),$$

$$\kappa_8^{\mp} = \left\{c'_{44}K_{4n}^{\pm} - c'_{24}\left(P_0 \pm np\right)\right\}\Pi_{4n}^{\pm} + c'_{34}K_{4n}^{\pm} - c'_{44}\left(P_0 \pm np\right),$$

$$\Phi_0^{\mp} = [\{c_{23}P_0K_0 \pm 2c_{24}npP_0 - c_{34}K_0^2 - 2c_{44}npK_0\}\Pi_0 - c_{33}K_0^2 \mp 2c_{34}npK_0 - c_{34}P_0K_0 \pm 2c_{44}npP_0]\xi_{\mp n},$$

$$\Phi_1^{\mp} = [\{-c_{23}P_0K_1 \pm 2c_{24}npP_0 - c_{34}K_1^2 \pm 2c_{44}npK_1\}\Pi_1 - c_{33}K_1^2 \mp 2c_{34}npK_1 - c_{34}P_0K_1 \pm 2c_{44}npP_0]\xi_{\mp n},$$

$$\Phi_2^{\mp} = [\{-c_{23}P_0K_2 \pm 2c_{24}npP_0 - c_{34}K_2^2 \pm 2c_{44}npK_2\}\Pi_2 - c_{33}K_2^2 \mp 2c_{34}npK_2 - c_{34}P_0K_2 \pm 2c_{44}npP_0]\xi_{\mp n},$$

$$\Phi_3^{\mp} = [\{c'_{23}P_0K_3 \pm 2c'_{24}npP_0 - c'_{34}K_3^2 \mp 2c'_{44}npK_3\}\Pi_3 - c'_{33}K_3^2 \mp 2c'_{34}npk_3 + c'_{34}P_0K_3 \pm 2c'_{44}npP_0]\xi_{\mp n},$$

$$\Phi_4^{\mp} = [\{c'_{23}P_0K_4 \pm 2c'_{24}npP_0 - c'_{34}K_4^2 \mp 2c'_{44}npK_4\}\Pi_4 - c'_{33}K_4^2 \mp 2c'_{34}npK_4 + c'_{34}P_0K_4 \pm 2c'_{44}npP_0]\xi_{\mp n},$$

$$\Phi_5^{\mp} = -\left[\left\{c_{23}\left(P_0 \pm np\right) + c_{34}K_{1n}^{\pm}\right\}\Pi_{1n}^{\pm} + c_{33}K_{1n}^{\pm} + c_{34}\left(P_0 \pm np\right)\right],$$

$$\Phi_6^{\mp} = -\left[\left\{c_{23}\left(P_0 \pm np\right) + c_{34}K_{2n}^{\pm}\right\}\Pi_{2n}^{\pm} + c_{33}K_{2n}^{\pm} + c_{34}\left(P_0 \pm np\right)\right],$$

$$\Phi_7^{\mp} = \left\{-c'_{23}\left(P_0 \pm np\right) + c'_{34}K_{3n}^{\pm}\right\}\Pi_{3n}^{\pm} + c'_{33}K_{3n}^{\pm} - c'_{34}\left(P_0 \pm np\right),$$

$$\Phi_8^{\mp} = \left\{-c'_{23}\left(P_0 \pm np\right) + c'_{34}K_{4n}^{\pm}\right\}\Pi_{4n}^{\pm} + c'_{33}K_{4n}^{\pm} - c'_{34}\left(P_0 \pm np\right).$$

The spectrum theorem (Abubakar 1963) which gives the relations between the angle of regular and irregular waves and the Snell law (Asano 1960) for obtaining the above Eq. (24) are given by

$$sin\theta_m^{\pm} - sin\theta_i = \pm\frac{np}{\omega}v_i, n = 0,1,2,\ ,i = 1,2,3,4, \tag{25}$$

and $$\frac{sin\theta_i}{v_i.\theta_i} = \frac{1}{v_a},\ i = 0,1,2,3,4 \tag{26}$$

where (+ve) and (−ve) signs on both side of (25) are corresponds to each other, v_a being the apparent velocity.

On solving Eq. (24), we get the amplitude ratios of the regularly reflected and transmitted waves and irregularly reflected and transmitted waves due to the incident wave as

$$\frac{\mathcal{B}_i}{\mathcal{B}_0}=\frac{\wedge_{\mathcal{B}_i}}{\wedge},\ \frac{\mathcal{B}_{in}^{\pm}}{\mathcal{B}_0}=\frac{\wedge_{\mathcal{B}_{in}^{\pm}}}{\wedge^{\pm}}, \tag{27}$$

where the values of $\{\wedge_{\mathcal{B}_i},\wedge_{\mathcal{B}_{in}^{\pm}}\}, i=1,2,3,4$ are obtained by replacing the first, second, third and fourth columns of $\{\wedge,\wedge^{\pm}\}$ with column matrices $\{\nabla,\nabla^{\mp}\}$ respectively.

ENERGY DISTRIBUTION

Let us consider the energy distribution between the reflected and transmitted waves as they interact with the plane interface, $x_3 = 0$. The rate of transmission of energy per unit area is given by (Achenback 1973)

$$E=<T_{23}.\dot{u}_2>+<T_{33}.\dot{u}_3>+<T_{23}^{'}.\dot{u}_2^{'}>+<T_{33}^{'}.\dot{u}_3^{'}>. \tag{28}$$

By using the displacement vectors of (16), (17), (18) and (19), and the stress tensors (1) into (28), the incident energy, the energy of reflected and transmitted *qSV* and *qP*-waves are given by

$$E_0=\omega l_0\mathcal{B}_0^2 e^{2i\xi K_0}e^{2i(\omega t-P_0 t)},$$

$$E=\omega l_i\mathcal{B}_i^2 e^{-2i\xi K_i}e^{2i(\omega t-P_0 t)}+\sum_{n=1}^{\infty}\omega l_i^{\pm}(\mathcal{B}_{in}^{\pm})^2 e^{\mp 2inpx_2}$$
$$e^{-2i\xi K_{in}^{\pm}}e^{2i(\omega t-P_0 t)},\ i=1,2,3,4 \tag{29}$$

where

$$l_0=(c_{24}\Pi_0^2+c_{44}\Pi_0+c_{23}\Pi_0+c_{34})P_0-(c_{44}\Pi_0^2+2c_{34}\Pi_0+c_{33})K_0,$$

$$l_i=\begin{cases}(c_{24}\Pi_i^2+c_{44}\Pi_i+c_{23}\Pi_i+c_{34})P_0+(c_{44}\Pi_i^2+2c_{34}\Pi_i+c_{33})K_i, & i=1,2\\ (c'_{24}\Pi_i^2+c'_{44}\Pi_i+c'_{23}\Pi_i+c'_{34})P_0-(c'_{44}\Pi_i^2+2c'_{34}\Pi_i+c'_{33})K_i, & i=3,4\end{cases}$$

$$l_i^{\pm}=\begin{cases}(c_{24}(\Pi_{in}^{\pm})^2+c_{44}\Pi_{in}^{\pm}+c_{23}\Pi_{in}^{\pm}+c_{34})(P_0\pm np)+(c_{44}(\Pi_{in}^{\pm})^2\\ +2c_{34}\Pi_{in}^{\pm}+c_{33})K_{in}^{\pm}, & i=1,2\\ (c'_{24}(\Pi_{in}^{\pm})^2+c'_{44}\Pi_{in}^{\pm}+c'_{23}\Pi_{in}^{\pm}+c'_{34})(P_0\pm np)-(c'_{44}(\Pi_{in}^{\pm})^2\\ +2c'_{34}\Pi_{in}^{\pm}+c'_{33})K_{in}^{\pm}, & i=3,4\end{cases}.$$

Now, from the above expressions of different energy, the energy ratios of regularly and irregularly reflected and transmitted waves due to the incident wave is given by

$$E_i=\left|\frac{l_i}{l_0}\right|\left|\frac{\mathcal{B}_i}{\mathcal{B}_0}\right|^2 \tag{30}$$

and $E_i^{\pm}=\left|\frac{l_i^{\pm}}{l_0}\right|\left|\frac{\mathcal{B}_{in}^{\pm}}{\mathcal{B}_0}\right|^2, \forall\ i=1,2,3,4.$ (31)

Here, $(E_i, E_i^{\pm})$ represents the energy ratios for regularly and irregularly reflected and transmitted *qSV* and *qP*-wave.

SPECIAL CASE

If the corrugated interface is represented by only one cosine term i.e. $x_3 = d\cos px_2$, with *d* as the amplitude of the corrugation, then we have

$$\xi_{\pm n}=\begin{cases}0, & if\ \ n\neq 1\\ \frac{d}{2}, & if\ \ n=1\end{cases}$$

The first order approximation of the amplitude ratios for irregularly reflected and transmitted waves using these values are obtained from Eq. (27) as follows

$$r_{i1}^{\pm}=\frac{\mathcal{B}_{i1}^{\pm}}{\mathcal{B}_0},\ i=1,2,3,4. \tag{32}$$

In the normal incidence, θ_0 = 0°, we obtain that $\cos\theta_{11}^{+}=\cos\theta_{11}^{-}$ and $\cos\theta_{21}^{+}=\cos\theta_{21}^{-}$ due to the Eqs. (25) and (26). Hence, the amplitude ratios for the irregularly reflection and transmission waves are related as follows

$$r_{i1}^{+}=r_{i1}^{-},\ i=1,2,3,4.$$

These outcomes are attributed to (Asano 1960) in relation to the relevant problem.

In the grazing angle of incidence, $\theta_0=\pi/2$, the amplitude ratios are given by Eq. (32) using the modifications given in the Appendix I. Then, the energy ratios are obtained from Eq. (31) by putting n=1.

PARTICULAR CASE

(a) Upon transforming the two monoclinic half-spaces, $\mathcal{M}$ and $\mathcal{M}'$, into transversely isotropic half-spaces, while aligning the axis of symmetry with the x-axis, we have

$$c_{12}=c_{13},\ c_{22}=c_{33},\ c_{55}=c_{66},\ c_{23}=c_{22}-2c_{44},$$
$$c_{14}=c_{24}=c_{34}=c_{56}=0,$$
$$c'_{12}=c'_{13},\ c'_{22}=c'_{33},\ c'_{55}=c'_{66},\ c'_{23}=c'_{22}-2c'_{44},$$
$$c'_{14}=c'_{24}=c'_{34}=c'_{56}=0$$

Using these values, the velocity equations can be expressed as follows:

$$v_1^2=\frac{\lambda+2\mu}{\rho},\ v_0^2=v_2^2=\frac{\mu}{\rho},\ v_3^2=\frac{\lambda'+2\mu'}{\rho'},\ v_4^2=\frac{\mu'}{\rho'}$$

These findings align with the principles of classical elasticity (Achenback 1973). Subsequently, the amplitude ratios are derived using the Eq. (27), incorporating the adjusted values provided in Appendix II. Similarly, the energy ratios associated with both regular and irregular waves are obtained using Eqs. (30) and (31), taking into account the modified values presented in Appendix III.

(b) When the interface corrugation is ignored, i.e., when $d = 0$, the problem simplifies to the interaction of elastic waves at a plane interface between two monoclinic elastic half-spaces. The energy ratios in this case correspond to the regularly reflected and transmitted waves and are described by Eq. (30).

(c) In the absence of the half-space $\mathcal{M}'$, the problem reduces only to the reflection of *qSV* and *qP* waves when an incident *qSV*-wave is considered. The energy ratios can be determined using Eq. (30), where the values are adjusted as follows

$$\wedge = y_1 z_2 - y_2 z_1,\ \wedge_{B_1} = y_2 z_0 - y_0 z_2,\ \wedge_{B_2} = y_0 z_1 - y_1 z_0$$

GEOMETRICAL INTERPRETATION

In the following section, we will analyse numerically the derived expressions for phase velocity and energy ratio, as discussed in the previous section. We take the following values of elastic constants and density for monoclinic medium (Singh and Lalvohbika 2018)

Table 1

For Half-space, $\mathcal{M}$ Lithium Tantalate			For Half-space, $\mathcal{M}'$ Lithium Tantalate		
c_{22}	2.33×10^{11}	Nm^{-2}	c'_{22}	2.03×10^{11}	Nm^{-2}
c_{23}	0.81×10^{11}	Nm^{-2}	c'_{23}	0.75×10^{11}	Nm^{-2}
c_{24}	0.11×10^{11}	Nm^{-2}	c'_{24}	-0.09×10^{11}	Nm^{-2}
c_{33}	2.75×10^{11}	Nm^{-2}	c'_{33}	2.45×10^{11}	Nm^{-2}
c_{34}	0	Nm^{-2}	c'_{34}	0	Nm^{-2}
c_{44}	0.94×10^{11}	Nm^{-2}	c'_{44}	1.06×10^{11}	Nm^{-2}
ρ	7400	Kgm^{-2}	ρ'	4700	Kgm^{-2}

To examine the effect of frequency parameters (ω/pv_0) and corrugated parameters (pd), we convert the parameters in dimensionless form by dividing with c_{44}. We consider a series of these parameters, (ω/pv_0) and (pd), to compare the variations of phase velocity and energy ratio with angle of incidence for the following series

ω/pv_0	80	90	100
pd	0.0001	0.0002	0.0003

Figure 1 represents the variation of velocities (v_1, v_2) and (v_3, v_4) for regularly reflected and transmitted waves respectively with respect to the angle of incidentce (θ_0). The findings reveal that the velocities of the transmitted waves are higher than those of the reflected waves at the same angle of incidence (θ_0). Furthermore, it is observed that the velocity of the *qP*-wave (v_1, v_3) exceeds those of the *qSV*-wave (v_2, v_4) for both reflection and transmission of wave propagation.

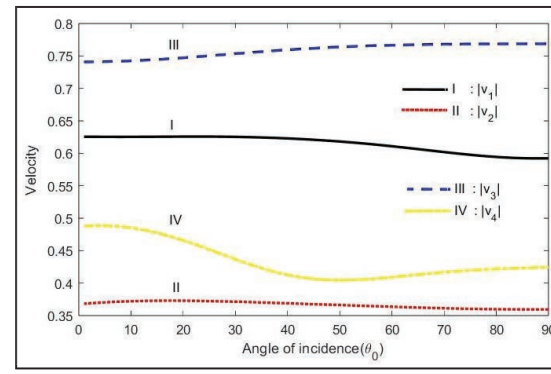

Fig. 1: Variation of Velocities with Respect to Angle of Incidence (θ_0).

Figure 2 depicts the variation of energy ratios ($|E_1|$, $|E_2|$), ($|E_3|$, $|E_4|$). for regularly reflected and transmitted *qSV* and *qP*-waves with respect to the angle of incidence (θ_0). The graph shows that initially, the values of $|E_1|$ and $|E_2|$ are nearly zero during the early stages of propagation. However, as θ_0 increases, they form parabolic curves. In the case of

transmitted waves, the energy ratio $|E_3|$ gradually decreases and reaches its minimum value around θ_0 = 85°. On the other hand, the energy ratio $|E_4|$ attains its minimum value at the grazing angle of incidence and approximately at 58°, and then rapidly increases as θ_0 continues to increase.

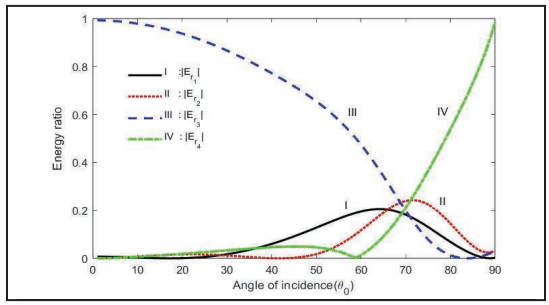

Fig. 2: Variation of Energy Ratios with Respect to Angle of Incidence (θ_0).

Effect of Frequency ω/pv_0 and Corrugation *pd* Parameters

By analysing Figs. 3 and 4, it can be observed that the energy ratios of irregularly reflected *qSV*-waves, namely $|E_1^+|$ and $|E_1^-|$, exhibit similar variations. These ratios increase as both the parameters ω/pv_0 and *pd* increase, with the influence of *pd* being more significant than ω/pv_0. In Figs. 3a and 3b, the energy ratio $|E_1^+|$ reaches its minimum value at the angles of incidence 15° and 84°, respectively. Similarly, in Figs. 4a and 4b, the energy ratio $|E_1^-|$ attains its minimum value at of 18° and 88°, respectively. The maximum effect of both parameters, ω/pv_0 and *pd*, occurs at 54° for $|E_1^+|$ and 58° for $|E_1^-|$, as illustrated in the figures.

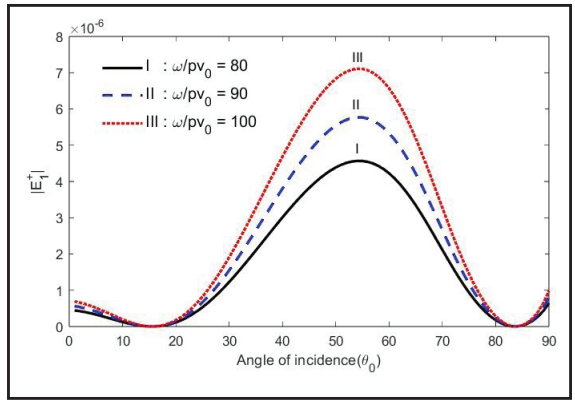

(a) Effect of ω/pv_0.

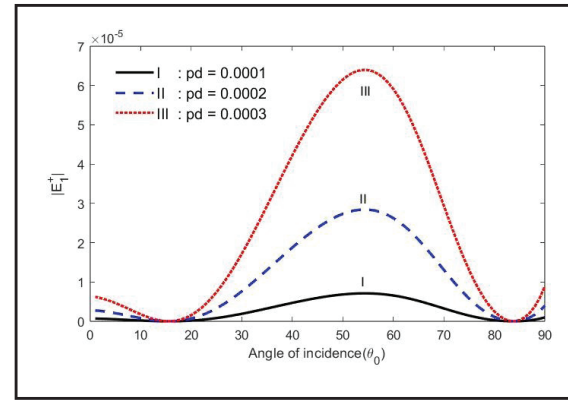

(b) Effect of *pd*.

Fig. 3: Variation of $|E_1^+|$ for Different Values of Parameters with (θ_0).

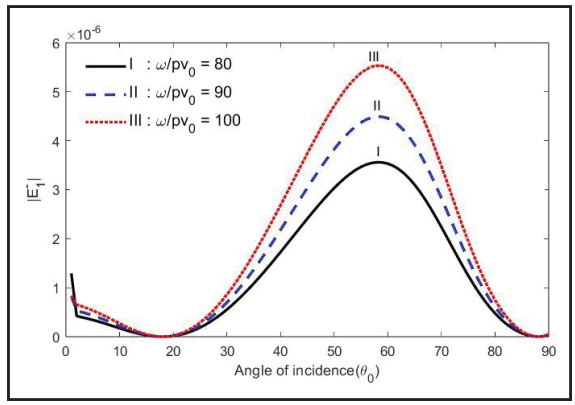

(a) Effect of ω/pv_0.

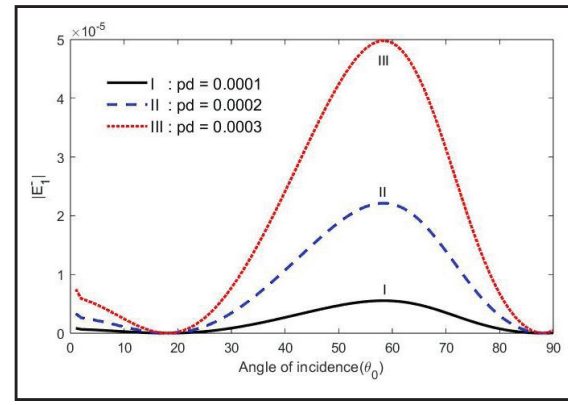

(b) Effect of *pd*.

Fig. 4: Variation of $|E_1^-|$ for Different Values of Parameters with (θ_0).

The analysis of Figs. 5 and 6 reveals an interesting pattern in the energy ratios of the irregularly reflected *qP*-waves, characterized by a corrugated nature. In Figs. 5a and 5b, the variation of $|E_2^+|$ exhibits a parabolic shape within the range of $0° < \theta_0 < 40°$ and $40° < \theta_0 < 90°$, while $|E_2^-|$ follows a similar pattern within the range of $2° < \theta_0 < 46°$ as shown in the Figs. 6a and 6b. The energy ratios increase as both ω/pv_0 and *pd* increase. Notably, $|E_2^+|$ reaches its minimum values at 0°, 40°, and 90°, while $|E_2^-|$ achieves its minimum values at 2° and 46°. In this variation, the parameter *pd* has a greater impact compared to ω/pv_0, and the maximum influence of both ω/pv_0 and *pd* occurs at 68° and 73° for $|E_2^+|$ and $|E_2^-|$ respectively.

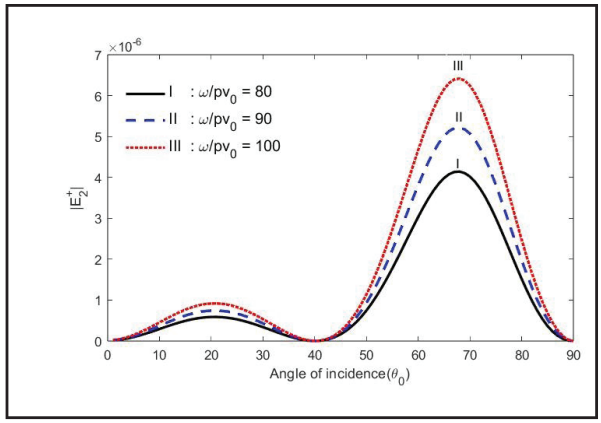

(a) Effect of ω/pv_0.

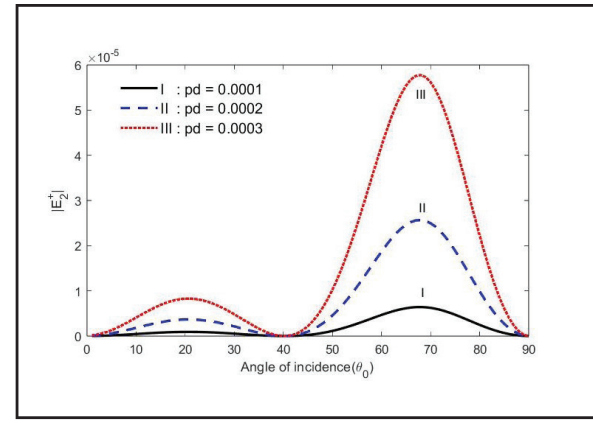

(b) Effect of *pd*.

Fig. 5: Variation of $|E_2^+|$ for Different Values of Parameters with (θ_0).

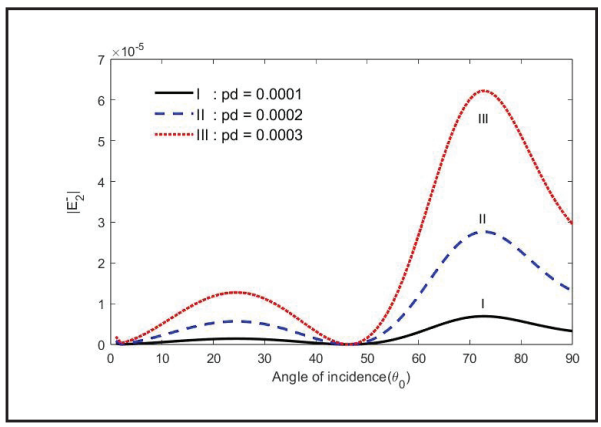

(a) Effect of ω/pv_0.

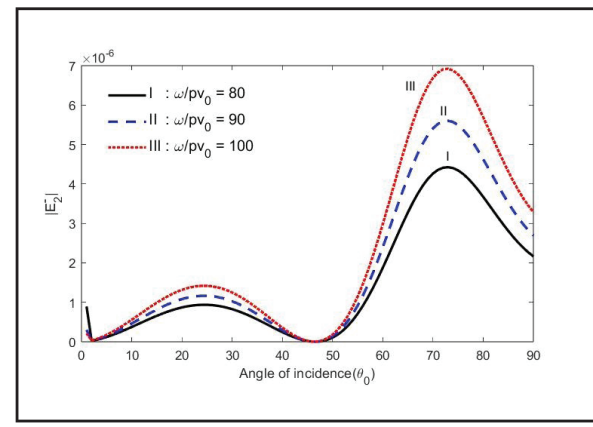

(b) Effect of *pd*.

Fig. 6: Variation of $|E_2^-|$ for Different Values of Parameters with (θ_0).

Figures 7 and 8 illustrate the variations in the energy ratios of the irregularly transmitted *qSV*-waves with respect to the angle of incidence. In Figs. 7a and 7b, the values of $|E_3^+|$ decrease beyond a certain point as θ_0 increases. A parabolic curve is formed within the range of $43° < \theta_0 < 73°$, and the minimum value of $|E_3^+|$ is observed at 43° and 73°. Subsequently, the curve increases as θ_0 increases, reaching its maximum value at the normal angle of incidence. In Figs. 8a and 8b, the curve of $|E_3^-|$ exhibits a sharp decrease within the range of $1° < \theta_0 < 3°$ and a gradual decrease in the range of $12° < \theta_0 < 55°$ and $67° < \theta_0 < 77°$. After these decrements, the curve increases for the rest of the interval of θ_0. Two peaks are observed at 12° and 67°, while two troughs are observed at 55° and 77°. From a comparative analysis of the curves represented by $|E_3^+|$ and $|E_3^-|$, it can be concluded that *pd* has a more significant effect than ω/pv_0, and the variation of these parameters is particularly influential at the initial stages of propagation.

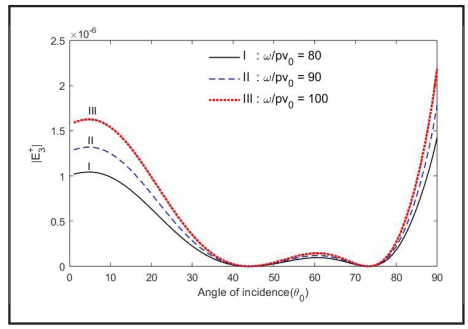

(a) Effect of ω/pv_0.

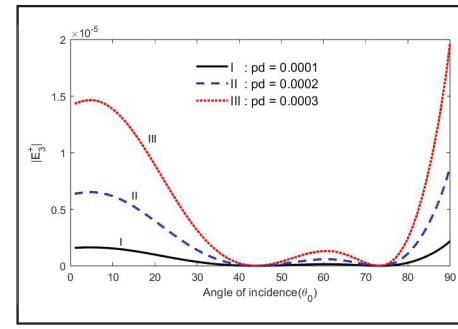

(b) Effect of *pd.*

Fig. 7: Variation of $|E_3^+|$ for Different Values of Parameters with (θ_0).

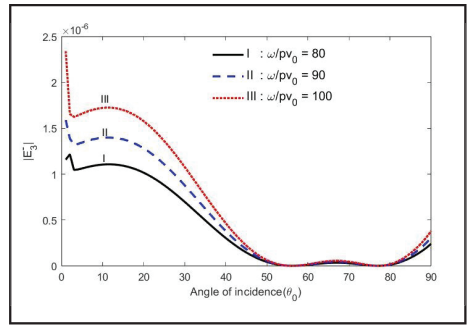

(a) Effect of ω/pv_0.

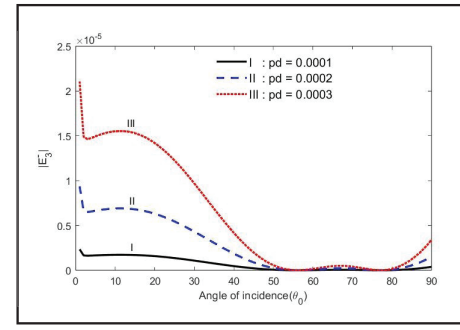

(b) Effect of *pd.*

Fig. 8: Variation of $|E_3^-|$ for Different Values of Parameters with (θ_0).

The energy ratios, $|E_4^+|$ and $|E_4^-|$, of the corrugated transmitted *qP*-waves show interesting variations with respect to the incident angle, θ_0, as depicted in Figs. 9 and 10. Notably, both ratios exhibit similar patterns, which are influenced by the parameters ω/pv_0 and *pd.* Analysing the behaviour of the ratio $|E_4^+|$ which was shown in Figs. 9a and 9b, it gradually increases as both ω/pv_0 and *pd* change, then forming a parabolic curve within the range of $15°<\theta_0<70°$. However, beyond this range, the ratio experiences a sudden increase as θ_0 further increases. Examining the values of $|E_4^-|$ in Figs. 10a and 10b, it is observed that these values rapidly decrease within a narrow interval of $1°<\theta_0<3°$. However, in the broader range of $3°<\theta_0<70°$, the curves of $|E_4^-|$ form a parabolic shape with changes in both ω/pv_0 and *pd*. Subsequently, there is a sharp increase in the ratio as θ_0 approaches the grazing angle of incidence. The above analysis reveals that the effect of *pd* is more significant than that of ω/pv_0, and both parameters have minimal influence at the initial stages of wave propagation.

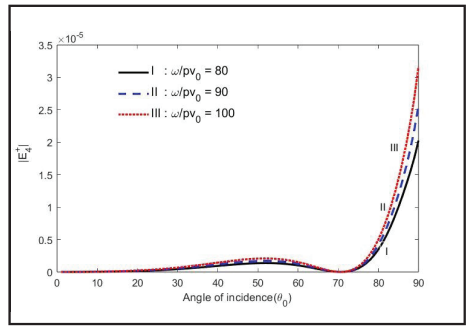

(a) Effect of ω/pv_0.

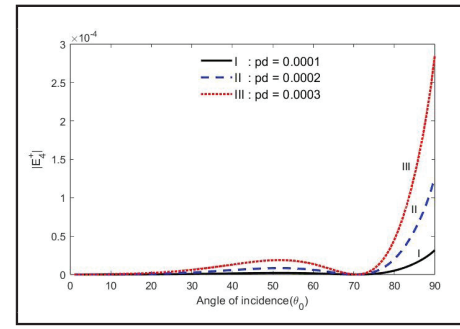

t(b) Effect of *pd.*

Fig. 9: Variation of $|E_4^+|$ for Different Values of Parameters with (θ_0).

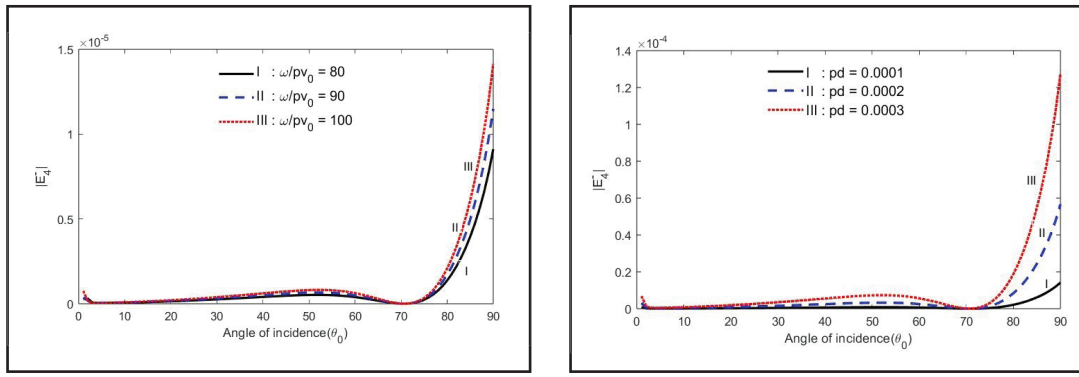

(a) Effect of ω/pv_0. **(b) Effect of *pd*.**

Fig. 10: Variation of $|E_4^-|$ for Different Values of Parameters with (θ_0).

In Fig. 11, the energy ratios corresponding to the regularly reflected and transmitted waves remain unaffected by changes in ω/pv_0 and *pd*. However, the energy ratios corresponding to the irregularly reflected and transmitted waves exhibit a nonlinear growth as ω/pv_0 and *pd* increase at different rates, as visually represented in Figs. 12 and 13.

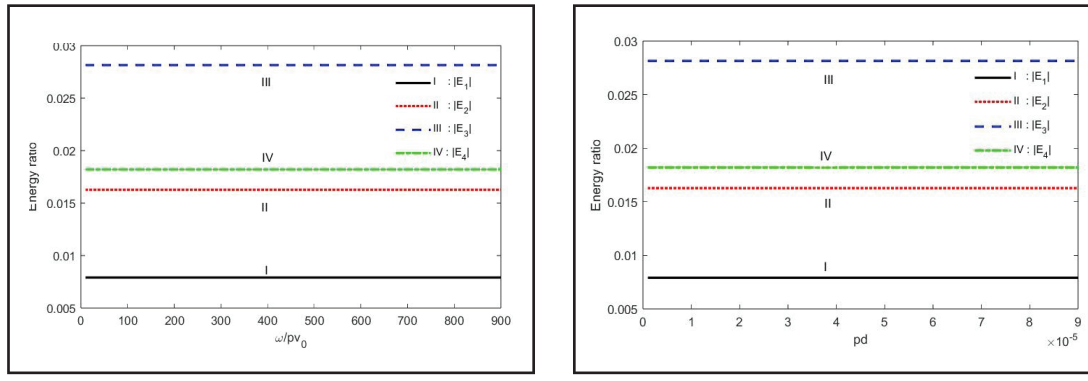

(a) **(b)**

Fig. 11: Variation of Energy Ratios of Regularly Reflected and Transmitted Waves with Respect to ω/pv_0 and *pd*.

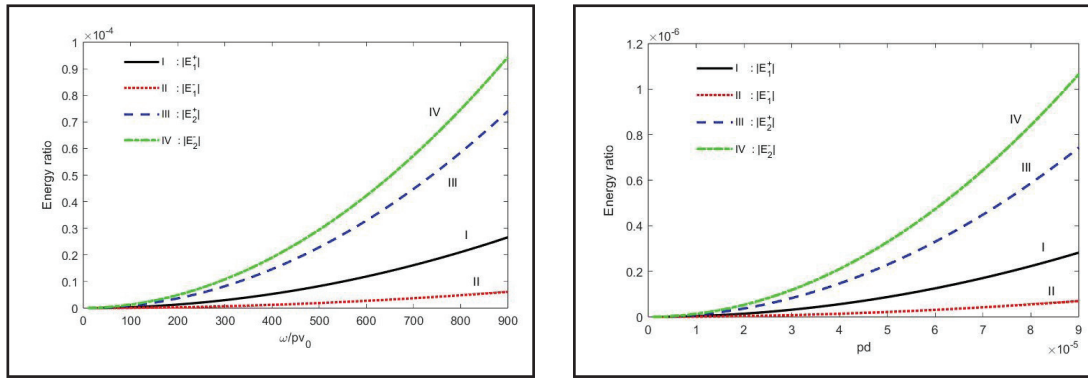

(a) **(b)**

Fig. 12: Variation of Energy Ratios of Irregularly Reflected Waves with Respect to ω/pv_0 and *pd*.

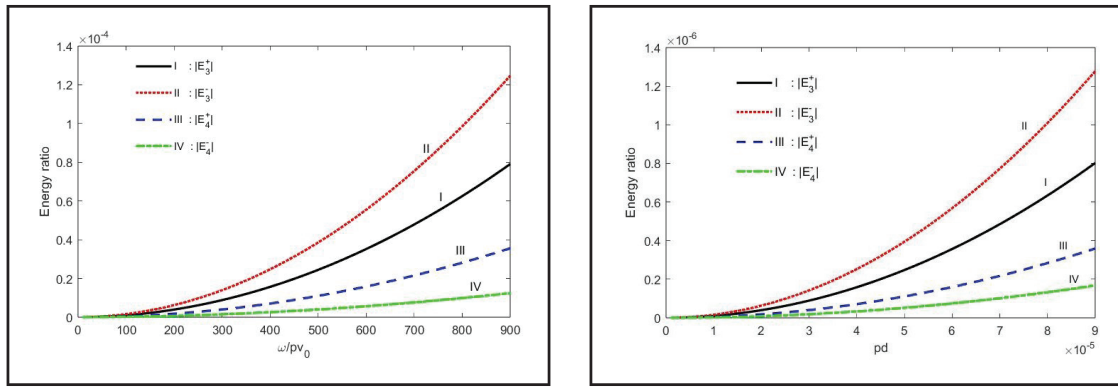

(a) (b)

Fig. 13: Variation of Energy Ratios of Irregularly Transmitted Waves with Respect to ω/pv_0 and *pd*.

CONCLUSION

The behaviour of elastic waves when a plane *qSV*-wave is incident upon a corrugated interface between two dissimilar monoclinic elastic half-spaces, each with different phase velocity are investigated. Rayleigh's method of approximation is employed to obtain the velocities and energy ratios for the regular and irregular reflection and transmission of *qSV*/*qP*-waves respectively. Numerical computations are performed for a specific model, enabling the examination of how the velocities and energy ratios change with variations in the frequency and corrugation parameters. The study discusses how these parameters affect the behaviour of elastic waves concerning reflection and transmission. The following conclusions can be drawn:

(i) The velocity and energy ratios are functions of several parameters, including the angle of incidence, elastic constants, corrugation, and frequency parameters.

(ii) Both theoretically and numerically, the velocities and energy ratios of regularly reflected and transmitted waves are independent of ω/pv and *pd*.

(iii) The energy ratios for irregularly reflected and transmitted waves increase with rising values of both ω/pv and *pd*.

(iv) The influence of pd on the irregularly reflected and transmitted waves is more significant than that of ω/pv.

(v) The energy ratios for irregular waves are observed to be relatively small.

APPENDIX I

$$y_0 = (\Pi_0 c_{24} + c_{44})P_0, \quad z_0 = (\Pi_0 c_{23} + c_{34})P_0,$$

$$\zeta_1^{\mp} = \iota\xi_{\mp 1}\sum_{i=1}^{4} K_i \frac{\mathcal{B}_i}{\mathcal{B}_0}, \quad \zeta_2^{\mp} = \iota\xi_{\mp 1}\sum_{i=1}^{4} \Pi_i K_i \frac{\mathcal{B}_i}{\mathcal{B}_0},$$

$$\zeta_3^{\mp} = \iota\left[\kappa_0^{\mp} + \kappa_1^{\mp}\frac{\mathcal{B}_1}{\mathcal{B}_0} + \kappa_2^{\mp}\frac{\mathcal{B}_2}{\mathcal{B}_0} - \kappa_3^{\mp}\frac{\mathcal{B}_3}{\mathcal{B}_0} - \kappa_4^{\mp}\frac{\mathcal{B}_4}{\mathcal{B}_0}\right],$$

$$\kappa_0^{\mp} = [\mp(c_{23} - c_{22})pP_0\Pi_0 \mp (c_{34} - c_{24})pP_0]\xi_{\mp 1},$$

$$\Phi_0^{\mp} = [\pm 2c_{24}pP_0\Pi_0 \pm 2c_{44}pP_0]\xi_{\mp 1}.$$

APPENDIX II

$$y_0 = c_{44}(P_0 - \Pi_0 K_0), \quad y_i = \begin{cases} c_{44}(P_0 + \Pi_i K_i), & i = 1,2 \\ c'_{44}(P_0 - \Pi_i K_i), & i = 3,4 \end{cases},$$

$$z_0 = c_{22}(\Pi_0 P_0 - K_0) - 2c_{44}\Pi_0 P_0,$$

$$z_i = \begin{cases} c_{22}(\Pi_i P_0 + K_i) - 2c_{44}\Pi_i P_0, & i = 1,2 \\ c'_{22}(\Pi_i P_0 - K_i) - 2c'_{44}\Pi_i P_0, & i = 3,4 \end{cases},$$

$$\zeta_1^{\mp} = \iota\xi_{\mp n}\left[-K_0 + \sum_{i=1}^{4} K_i \frac{\mathcal{B}_i}{\mathcal{B}_0}\right],$$

$$\zeta_2^{\mp} = \iota\xi_{\mp n}\left[-\Pi_0 K_0 + \sum_{i=1}^{4} \Pi_i K_i \frac{\mathcal{B}_i}{\mathcal{B}_0}\right],$$

$$\zeta_3^{\mp} = \iota\left[\kappa_0^{\mp} + \kappa_1^{\mp}\frac{\mathcal{B}_1}{\mathcal{B}_0} + \kappa_2^{\mp}\frac{\mathcal{B}_2}{\mathcal{B}_0} - \kappa_3^{\mp}\frac{\mathcal{B}_3}{\mathcal{B}_0} - \kappa_4^{\mp}\frac{\mathcal{B}_4}{\mathcal{B}_0}\right],$$

$$\zeta_4^{\mp} = \iota\left[\Phi_0^{\mp} + \Phi_1^{\mp}\frac{\mathcal{B}_1}{\mathcal{B}_0} + \Phi_2^{\mp}\frac{\mathcal{B}_2}{\mathcal{B}_0} - \Phi_3^{\mp}\frac{\mathcal{B}_3}{\mathcal{B}_0} - \Phi_4^{\mp}\frac{\mathcal{B}_4}{\mathcal{B}_0}\right],$$

$$\kappa_0^{\mp} = [\{\pm 2c_{44}npP_0 - c_{44}K_0^2\}\Pi_0 \pm 2c_{44}npK_0 + c_{44}P_0K_0]\xi_{\mp n},$$

$$\kappa_i^{\mp} = \begin{cases} \left(\{\pm 2c_{44}npP_0 - c_{44}K_i^2\}\Pi_i \mp 2c_{44}npK_i - c_{44}P_0K_i\right)\xi_{\mp n}, & i = 1,2 \\ \left(\{\pm 2c'_{44}npP_0 - c'_{44}K_i^2\}\Pi_i \pm 2c'_{44}npK_i + c'_{44}P_0K_i\right)\xi_{\mp n}, & i = 3,4 \end{cases},$$

$$\kappa_j^{\mp} = \begin{cases} -c_{44}\left\{K_{in}^{\pm}\Pi_{in}^{\pm} + P_0 \pm np\right\}, & j = 5,6, i = 1,2 \\ c'_{44}\left\{K_{in}^{\pm}\Pi_{in}^{\pm} - P_0 \mp np\right\}, & j = 7,8, i = 3,4 \end{cases},$$

$$\Phi_0^{\mp} = [\{(c_{22} - 2c_{44})P_0K_0 - 2c_{44}npK_0\}\Pi_0 - c_{22}K_0^2 \pm 2c_{44}npP_0]\xi_{\mp n}$$

$$\Phi_i^{\mp} = \begin{cases} \left(\{(2c_{44} - c_{22})P_0K_i \pm 2c_{44}npK\}\Pi_i - c_{22}K_i^2 \pm 2c_{44}npP_0\right)\xi_{\mp n}, i = 1,2 \\ \left(\{(c'_{22} - 2c'_{44})P_0K_i \mp 2c'_{44}npK_i\}\Pi_i - c'_{22}K_i^2 \pm 2c'_{44}npP_0\right)\xi_{\mp n}, i = 3,4 \end{cases},$$

$$\Phi_j^{\mp} = \begin{cases} -[c_{22} - 2c_{44})(P_0 \pm np)\Pi_{in}^{\pm} + c_{22}K_{in}^{\pm}], & j = 5,6, i = 1,2 \\ (2c'_{44} - c'_{22})(P_0 \pm np)\Pi_{in}^{\pm} + c'_{22}K_{in}^{\pm}, & j = 7,8, i = 3,4 \end{cases}$$

Appendix III

$$l_0 = (c_{22} - c_{44})P_0\Pi_0 - c_{44}K_0\Pi_0^2 - c_{22}K_0,$$

$$l_i = \begin{cases} (c_{22} - c_{44})P_0\Pi_i + c_{44}K_i\Pi_i^2 + c_{22}K_i, & i = 1,2 \\ (c'_{22} - c'_{44})P_0\Pi_i - c'_{44}K_i\Pi_i^2 - c'_{22}K_i, & i = 3,4 \end{cases},$$

$$l_i^{\pm} = \begin{cases} (c_{22} - c_{44})(P_0 \pm np)\Pi_{in}^{\pm} + c_{44}K_{in}^{\pm}(\Pi_{in}^{\pm})^2 + c_{22}K_{in}^{\pm}, & i = 1,2 \\ (c'_{22} - c'_{44})(P_0 \pm np)\Pi_{in}^{\pm} - c'_{44}K_{in}^{\pm}(\Pi_{in}^{\pm})^2 - c'_{22}K_{in}^{\pm}, & i = 3,4 \end{cases}.$$

ACKNOWLEDGEMENTS

The authors J. Lalvohbika and R. Lianngenga acknowledged the Science and Engineering Research Board (SERB) for the financial assistance through Grant No. CRG/2021/000083 and No. EEQ/2021/000011 to complete this research work.

REFERENCES

Abubakar I (1962) Scattering of plane elastic waves at rough surfaces-I. Math Proc Camb Philos Soc 58:136-157.

Abubakar I (1963) Scattering of plane elastic waves at rough surfaces-II. Math Proc Camb Philos Soc 59:231-248.

Achenback JD (1973) Wave propagation in elastic solids. North-Holland Ser Appl Math Mech

Asano S (1960) Reflection and refraction of elastic waves at a corrugated boundary interface Part-I. The case of incidence of SH-wave. Bull Earthqu Res Inst 38:177-197.

Asano S (1961) Reflection and refraction of elastic waves at a corrugated boundary interface. Part-II. Bull Earthqu Res Inst 39:367-466.

Chattopadhyay A, Choudhury S (1995) The reflection phenomena of P-waves in a medium of monoclinic type. Int J Eng Sci 33:195-207.

Chattopadhyay A, Saha S (1996) Reflection and refraction of P waves at the interface of two monoclinic media. Int J Eng Sci 34:1271-1284.

Chattopadhyay A, Saha S, Chakraborty M (1996) The reflection of SV-waves in a monoclinic medium. Indian J Pure Appl Math 27:1029-1042.

Gupta S, Das SK, Pramanik S (2022) Reflection and transmission phenomena of SH waves in fluid saturated porous medium with corrugated interface. Mech Adv Mater Struct 29:5122-5141.

Hermans AJ (2003) Interaction of free-surface waves with a floating dock. J Eng Math 45:9-53.

Kaur J, Tomar SK (2004) Reflection and refraction of SH-waves at a corrugated interface between two monoclinic elastic half-spaces. Int J Numer Anal Methods Geomech 28:1543-1575.

Lalvohbika J, Singh SS (2019) Effect of corrugation on incident qP/qSV-waves between two dissimilar nematic elastomers. Acta Mech 230:3317-3338.

Lalvohbika J, Singh SS (2022) Scattering of qSH-waves from a corrugated interface between two dissimilar nematic elastomers. Waves Rand Compl Med 32:19-42.

Lay T, Wallace TC (1995) Modern global seismology. Elsevier.

Levy A, Deresiewicz H (1967) Reflection and transmission of elastic waves in a system of corrugated layers.BSSA 57:393-419.

Mandal BN, Das P (1996) Oblique diffraction of surface waves by a submerged vertical plate. J Eng Math 30:459-470.

Mciver M, Urka U (1995)Wave scattering by circular are shaped plates. J Eng Math 29:575-589.

Nayfeh AH(1991) Elastic wave reflection from liquid-anisotropic substrate interfaces. Wave motion 14:55-67.

Paul A, Campillo M (1988) Diffraction and conversion of elastic waves at a corrugated interface. Geophysics 53:1415-1424.

Pandit DK, Kundu S, Gupta S (2017) Analysis of dispersion and absorption characteristics of shear waves in sinusoidally corrugated elastic medium with void pores. R Soc Open Sci 4:160511.

Prasad B, Pal PC, Kundu S (2017) Propagation of SH-waves through non planer interface between visco-elastic and fibre-reinforced solid half-spaces. J Mech 33:545-557.

Pujol J (2003) Elastic wave propagation and generation in seismology. Cambridge: Cambridge University Press 227.

Rayleigh L (1907) On the dynamical theory of gratings. Proc R soc Lond Series A 79:399-416.

Rice SO (1951) Reflection of electromagnetic waves from slightly rough surfaces. Commun Pure Appl Math 4:351-378.

Saha S, Singh AK, Chattopadhyay A (2020) Analysis of reflection and refraction of plane wave at the separating interface of two functionally graded incompressible monoclinic media under initial stress and gravity. Eur Phys J Plus 135:1-31.

Sato R (1955) The reflection of elastic waves on corrugated surfaces. J Seismol Soc Jpn 8:8-22.

Singh P, Singh AK, Chattopadhyay A (2020) Reflection and transmission of thermoelastic waves at the corrugated interface of crystalline structure. J Therm Stresses 44:469-512.

Singh SJ (1999) Comments on 'The reflection phenomena of P-waves in a medium of monoclinic type' by Chattopadhyay and Choudhury. Int J Eng Sci 37:407-410.

Singh SJ, Khurana S (2001) Reflection and transmission of P and SV waves at the interface between two monoclinic elastic half-spaces. PNAS 71:305-320.

Singh SS, Lalvohbika J (2018) Response of corrugated interface on incident qSV-wave in monoclinic elastic half-spaces. Int J Appl Mech 23:727-750.

Singh SS, Tomar SK (2007) Quasi-P-waves at a corrugated interface between two dissimilar monoclinic elastic half-spaces. Int J Solids Struct 44:197-228.

Singh SS, Tomar SK (2008) qP-wave at a corrugated interface between two dissimilar prestressed elastic half-spaces. J Sound Vib 317:687-708.

Tomar SK, Kaur J (2003) Reflection and transmission of SH-waves at a corrugated interface between two laterally and vertically heterogeneous anisotropic elastic solid half-spaces. EPS 55:531-547.

Tomar SK, Kaur J (2007) Shear waves at a corrugated interface between anisotropic elastic and visco-elastic solid half-spaces. J Seismol 11:235-258.

Yu CW, Dravinski M (2009) Scattering of plane harmonic P, SV or Rayleigh waves by a completely embedded corrugated cavity. Geophys J Int 178:479-487.